Acta Chemica Scandinavica, 1995: 49: 676–682
Printed in Belgium – all rights reserved

Copyright © Acta Chemica Scandinavica 1995
ACTA
CHEMICA SCANDINAVICA
ISSN 0904–213X

Transition States in the Crystalline Phase? Thermal Rearrangements of Solid 4*H*-1,2,4-Triazoles

Per H. J. Carlsen,[a,†] Kåre B. Jørgensen,[a] Odd Reidar Gautun,[a] Susan Jagner[b] and Mikael Håkansson[b]

[a]Institute of Organic Chemistry, University of Trondheim-NTH, N-7034 Trondheim, Norway and [b]Department of Inorganic Chemistry, Chalmers University of Technology, S-412 96 Göteborg, Sweden

Carlsen, P. H. J., Jørgensen, K. B., Gautun, O. R., Jagner, S. and Håkansson M., 1995. Transition States in the Crystalline Phase? Thermal Rearrangements of Solid 4*H*-1,2,4-Triazoles. – Acta Chem. Scand. 49: 676–682 © Acta Chemica Scandinavica 1995.

In the crystalline state the 4-methyl and 4-ethyl substituted 4*H*-1,2,4-triazoles were found to undergo thermal rearrangement to the corresponding 1-alkyl substituted triazoles. The same reaction took place in the melts. Reaction rates were measured in both phases, and the activation parameters determined. The methyl substituted triazole reacted faster than the ethyl compound (methyl: E_a 104 kJ mol^{-1} vs. ethyl E_a 173 kJ mol^{-1}). The results were in agreement with a nucleophilic-type group transfer mechanism. The activation parameters for reactions in the solid state could be correlated with the interatomic distances between the 1-N atoms of the triazole rings and the α-atom of the 4-alkyl groups in a neighboring molecule.

Mechanistic studies of the thermal rearrangements of 4-alkyl substituted 4*H*-1,2,4-triazoles, **1**, to the corresponding 1-alkyl-1*H*-1,2,4-triazoles, **2**, have revealed[1] that the reaction probably proceeds via an initial nucleophilic S_N2-type displacement reaction according to which two alkyltriazole molecules form a dialkyltriazolium triazolate salt. Reaction of the dialkyltriazolium ion either with the anion or a neutral alkyltriazole subsequently yields the 1-alkyltriazole product molecule, Scheme 1. The rearrangement reactions were usually performed in a melt of the neat triazoles at temperatures of 270–300 °C. A more extensive mechanistic investigation of this problem will be reported shortly.

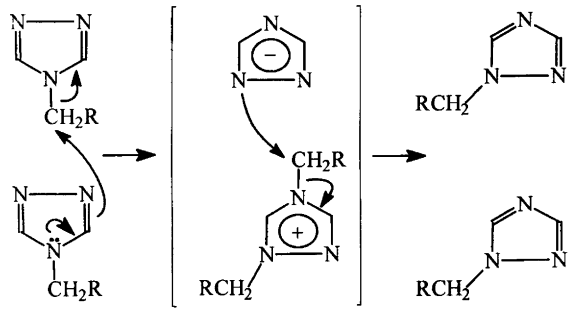

Scheme 1.

Results and discussion

The structures of a number of 1- and 4-substituted triazoles have been investigated by X-ray crystallography.[2] One of these was 4-ethyl-3,5-diphenyl-4*H*-1,2,4-triazole,[3] **3**. Inspection of the crystal structure of **3**, Fig. 1, revealed that the N(1) atom of one triazole molecule was in close proximity to the α-carbon of the 4-ethyl group of a neighboring triazole molecule, resembling the transition state of the S_N2 mechanism. Thus, considering the proposed mechanism for the rearrangement, we would actually expect that a rearrangement reaction may take place in the solid, crystalline state. The reactivity of organic compounds in the solid state is a subject of increasing interest as the posibility that reactions in the rigid structure of the solid state could be a way to simulate orientation-dependent catalytic effects. The subject has been treated in a couple of recent review papers.[4] Examples of S_N2-type mechanisms in the solid state have also been reported previously.[5] Indeed, thermolysis of **3** at temperatures well below the m.p. (m.p. 160–161 °C), clearly confirmed that the rearrangement reaction actually took place. We therefore undertook a detailed investigation of the thermolysis of **3**. This work included a study of the kinetics of the rearrangement in the crystalline state as well as in the melt. The product composition was easily determined by GLC analysis. It was possible to achieve an approximately 10–15% conversion before the crystals started to

† To whom correspondence should be adressed.

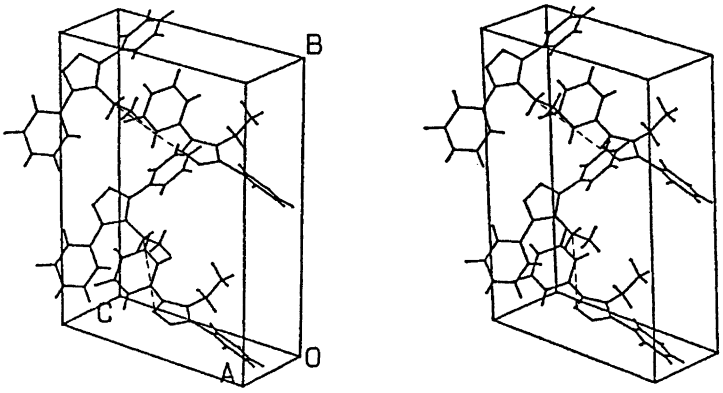

Fig. 1. Stereographic view of the crystal structure of 4-ethyl-3,5-diphenyl-4*H*-1,2,4-triazole, **3**.

melt. Later we found that 4-methyl-3,5-diphenyl-4*H*-1,2,4-triazole, **4**, also rearranged in the crystalline state. This indicated that **4** should exhibit crystal structural features similar to those at **3**, and we therefore undertook an X-ray crystallographic investigation of this compound.

Crystal structure analysis. Crystal data. 4-Methyl-3,5-diphenyl-4*H*-1,2,4-triazole, **4**, was synthesized according to a general procedure reported previously.[6] Single crystals were grown from toluene solution by slow evaporation at room temperature. They were colorless and of irregular prismatic shape. Crystal sizes of a few millimeters were obtained. Molecular formula, $C_{15}H_{13}N_3$, $M_r = 235.3$, orthorhombic, space group *Pnma*, $a = 11.345(5)$, $b = 26.057(2)$, $c = 4.057(2)$ Å, $V = 1199.2(8)$ Å^3, $Z = 4$, $D_{calcd} = 1.30$ g cm^{-3}, $\mu(\text{MoK}\alpha) = 0.74$ cm^{-1}, crystal dimensions $0.20 \times 0.30 \times 0.70$ mm, $F(000) = 496$. Diffracted intensities $(+h, +k, +l)$ from a crystal with the approximate dimensions $0.20 \times 0.30 \times 0.70$ mm were measured at 22 °C, with a Rigaku AFC6R diffractometer using graphite-monochromated MoKα radiation from an RU200 rotating anode operated at 9 kW (50 kV, 180 mA), for $5 < 2\theta < 50°$. The ω scan mode was employed with an ω scan rate of 16 °min^{-1} and a scan width of $(0.80 + 0.30\tan\theta)°$. Weak reflections $[I < 10\sigma(I)]$ were rescanned up to three times and counts accumulated to improve counting statistics. Stationary background counts were recorded on each side of the reflection. The ratio of peak counting time *vs.* background counting time was 2:1. Of the 1309 independent reflections measured, 513 had $I > 3\sigma(I)$ and were regarded as being observed. That the crystal was not subject to decay during measurement of intensities was checked by monitoring three reflections at regular intervals (after measurement of 150 reflections). Intensity data were corrected for Lorentz and polarization effects but not for absorption. Unit-cell parameters were obtained from diffractometer setting angles for 25 reflections in the range $20.2° < 2\theta < 34.9°$.

Structure determination and refinement. The structure was solved by direct methods (MITHRIL).[7] Full-matrix least-squares refinement of positional and anisotropic thermal parameters for non-hydrogen atoms gave a final $R = 0.037$, $R_w = 0.041$ for 85 parameters and 513 reflections, hydrogen atoms being included as a fixed contribution in calculated positions. Atomic scattering factors were taken from the literature,[8] and the F_o values were weighted according to $w = [\sigma^2(F_o)]^{-1}$. A final difference map showed a max., min. residual density of 0.11 and -0.15 Å^{-3}, respectively. All calculations were carried out with the TEXAN program system.[9]

Molecular and crystal structure of **4**. The molecular structure is illustrated in Fig. 2. The bond lengths (Å) and angles (°) in the molecule are listed in Tables 2 and 3, together with standard deviations. A stereographic view of the crystal structure of **4** is shown in Fig. 3. The angle

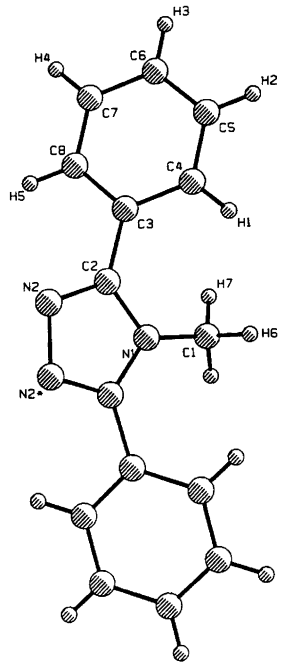

Fig. 2. View of the molecular structure of 4-methyl-3,5-diphenyl-4*H*-1,2,4-triazole, **4**.

Table 1. Fractonal atomic parameters for the non-hydrogen atoms for **4** with estimated standard deviations in parentheses. B_{eq} is defined as $(8\pi^2/3)\Sigma_i\Sigma_j U_{ij}a_i^*a_j^*a_ia_j$.

Atom	x	y	z	B_{eq}
N(1)	0.3678(2)	1/4	0.5344(8)	2.8(1)
N(2)	0.5340(2)	0.27682(7)	0.3100(6)	3.7(1)
C(1)	0.2594(3)	1/4	0.730(1)	3.3(2)
C(2)	0.4337(2)	0.2916(1)	0.4450(7)	3.0(1)
C(3)	0.3996(2)	0.3455(1)	0.4907(7)	3.0(1)
C(4)	0.2876(2)	0.3631(1)	0.4067(8)	3.8(1)
C(5)	0.2605(3)	0.4145(1)	0.4388(9)	4.4(2)
C(6)	0.3430(3)	0.4486(1)	0.553(1)	4.9(2)
C(7)	0.4538(3)	0.4316(1)	0.6392(9)	4.9(2)
C(8)	0.4822(3)	0.3802(1)	0.6070(8)	4.1(2)

Table 2. Selected interatomic distances (in Å). Estimated standard deviations in the least significant figure are given in parentheses.

Atom	Atom	Distance
N(1)	C(1)	1.464(5)
N(1)	C(2)	1.365(3)
N(2)	N(2)[a]	1.398(4)
N(2)	C(2)	1.320(3)
C(2)	C(3)	1.470(3)
C(3)	C(4)	1.393(4)
C(3)	C(8)	1.385(4)
C(4)	C(5)	1.381(4)
C(5)	C(6)	1.372(4)
C(6)	C(7)	1.378(4)
C(7)	C(8)	1.383(4)

[a] Symmetry code: x, $1/2-y$, z.

Table 3. Bond angles (in °) with estimated standard deviations in parentheses.

Atom	Atom	Atom	Angle
C(1)	N(1)	C(2)[a]	127.2(2)
C(2)	N(1)	C(2)[a]	105.0(3)
N(2)[a]	N(2)	C(2)	106.9(1)
N(1)	C(2)	N(2)	110.6(1)
N(1)	C(2)	C(3)	125.6(2)
N(2)	C(2)	C(3)	123.9(3)
C(2)	C(3)	C(4)	121.6(2)
C(2)	C(3)	C(8)	119.3(2)
C(4)	C(3)	C(8)	119.0(2)
C(3)	C(4)	C(5)	120.0(3)
C(4)	C(5)	C(6)	120.6(3)
C(5)	C(6)	C(7)	119.9(3)
C(6)	C(7)	C(8)	120.0(3)
C(3)	C(8)	C(7)	120.5(3)

[a] Symmetry code: x, $1/2-y$, z.

between the least-squares planes through the phenyl and the triazole ring is 45°.

Transition state geometries in the crystals? Assuming that the rearrangements of **3** as well as of **4** in the crystalline state proceed via similar mechanisms as in the melts, an important feature in the crystal structures is the distances and the alignment of the groups participating in the S_N2-type reactions, i.e., the 1-nitrogen atom of the triazole ring and the α-carbon atom of the 4-alkyl substituent of the neighboring molecule, Fig. 4. By inspection of the crystal structures, e.g., by the stereographic representations in Fig. 1 and 3, we found that in both cases the N(I)-atom was relatively close to the neighboring alkyl α-carbon. The distances and the angle described by the atoms around the α-carbon, $\measuredangle N(IV)_B-C(\alpha)_B-N(I)_A$, were calculated from the crystal structure data and are listed in Table 4. Indices A and B refer to the molecules shown in Fig. 4. The roman numbers refer to the numbering of the atoms in the individual molecules. In the crystals of **3** the molecules are aligned in layers parallel to the *ab*-plane, with their long axis alternating by ca. 90° as one moves from layer to layer along the *c*-axis. Within each layer molecules form 'head-to-tail' chains, running along the [310] and [3$\bar{1}$0], respectively, (Fig. 5). The $N(I)_A$-atom is aligned with the $C(\alpha)_B$-atom 4.6 Å away. The $N(IV)_B-C(\alpha)_B-N(I)_A$ angle is 161°. The crystal structure of **4** exhibited similar features with layers perpendicular to the *ac*-plane. Within each layer the molecules formed 'head-to-tail chains', however, of alternating orientation, (Fig. 3). The distance between the $N(I)_A$ atom and the $C(\alpha)_B$ atom was only 3.2 Å and the $N(IV)_B-C(\alpha)_B-N(I)_A$ angle was 167°. For both **3** and **4** the $N(IV)_B-C(\alpha)_B-N(I)_A$ atoms were close to the linear alignment needed for the proposed S_N2-like transition state. The intermolecular contacts along the 'chains' were close to the van der Waals type. The sum of the VdW radii for N and CH_3 (and CH_2) is ca. 3.5 Å. This readily allows for intermolecular group transfer. Thus, the orientation in the crystals is directly implicated in lowering the enthropy of activation, therefore facilitating the reaction in the crystal.

Kinetics. We next undertook a kinetic investigation of the thermolysis of **3** and **4** in the crystalline state as well as in the melts.

Experimental

General. As both sample holder and heat sink, a metal block was used (6 × 6 × 7 cm) with bore holes into which the capillary tubes closely fitted. The block was mounted in a Heraeus VZ 100 oven. Temperatures were measured

Table 4. Interatomic distances (in Å) and angles (in °) between the alkyl α-atom and the ring N-atoms in the crystal structures of compounds **3** and **4** (Fig. 4).

Compound	Distance/Å $C(\alpha)_B-N(I)_A$	Angle/° $N(I)_A-C(\alpha)_B-N(IV)_B$
3 (ethyl)[a]	4.609(9)	161.1(4)
4 (methyl)[b]	3.242(5)	167.1(8)

[a] Symmetry code for the ring N atoms (1) in Fig. 4: $x-1/2$, $1/2-y$, $z-1/2$. [b] Symmetry code for the ring N atoms (1) in Fig. 4: $x-1/2$, $1/2-y$, $1.5-z$ and $x-1/2$, y, $1.5-z$.

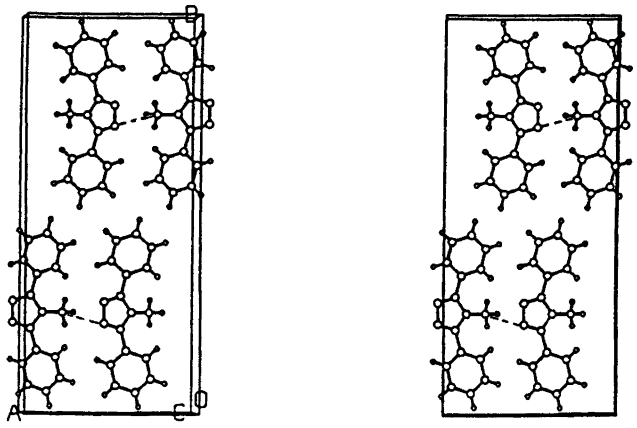

Fig. 3. Stereographic view of the crystal structure of 4-methyl-3,5-diphenyl-4*H*-1,2,4-triazole, **4**.

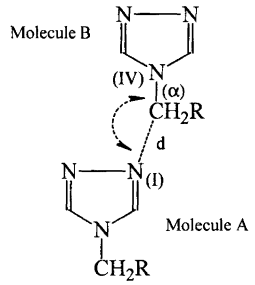

Fig. 4. Intramolecular distances between the ring-N and alkyl α-carbon atoms in relation to S_N2-type transition states.

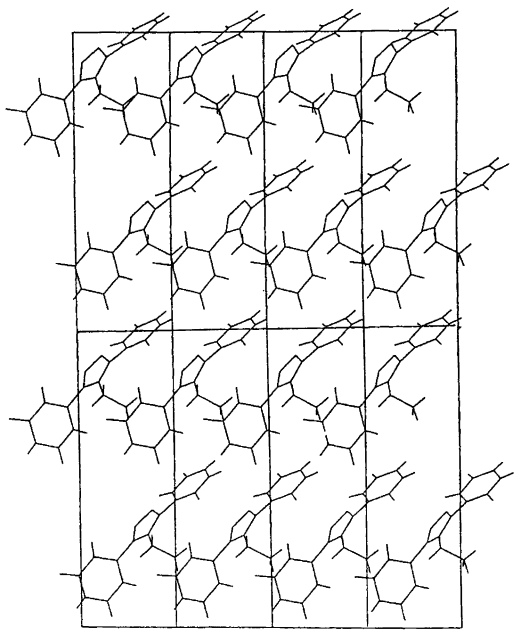

Fig. 5. The molecular packing of **3** viewed along the *c*-axis showing the formation of chains in a layer parallel with the *ab*-plane.

using a thermocouple probe (Chromel vs. Constantan) inserted into the middle of the metal block. The thermocouple probe was connected to a Cole–Parmer Instrument Co. model 8530 thermometer. The thermocouple probe was calibrated in ice–water (measured $-1\,°C$) and in boiling nonadecane (b.p. 330 °C, measured 327 °C). Owing to variations in the net-power a slight cyclic variation of the temperature was observed, ($\pm 2\,°C$). Thus, temperatures used in the calculations are average temperatures.

GLC measurements were performed on a Perkin-Elmer Autosystem Gas Chromatograph, equipped with an autosampler and a CP-SIL5-CB capillary column (25 m).The identities of the products were established by comparison of the spectroscopic and chromatographic properties with those of authentic samples.

The kinetic experiments for each compound were performed by exposing a number of separate samples to the thermolysis at a certain temperature. Thus, samples consisting of 4–5 mg triazole in sealed capillary tubes (o.d. 1.3–1.5 mm) were inserted into the sample holder (heat sink). The use of capillary tubes was necessary to avoid sublimation and to eliminate reactions with air. The metal block was heated in advance to the desired temperature in the oven. It took 30 s to insert all samples. Correction was made for the time delay when experiments lasted less than 1 h. At certain intervals capillary tubes were removed and dropped into cold water in order to terminate the reactions. The sample tubes were then crushed and the content dissolved in 2 ml of dichloromethane and subsequently analyzed by GLC analysis. As addition of other compounds would affect the crystals, internal standard techniques were not used. Concentrations were determined from experimental calibration curves of 1-alkyltriazole vs. 4-alkyltriazole. The measured molar fractions of product and reactant in the samples were used for the calculation of rate constants in the crystals as well as in the melts.

The first problem to address in this investigation, was to establish the kinetic rate law. Taking the proposed S_N2 type mechanism into account, second-order kinetics may be the logical choice. Thus, the experimental data were correlated to second-order kinetics, but the fit was not convincing. The plots of the inverse molar fraction of the

triazole vs. time exhibited a systematic positive curvature. The reason may be that (a) the reaction did not proceed via a bimolecular mechanism, (b) it followed pseudo-first-order kinetics, (c) the kinetic model breaks down in the rigid concentrated environment of the crystals or melts or (d) the curvature was an indication for an autocatalytic reaction. However, from a kinetic point of view it may not make much sense to discuss concentrations, activities or molecularity in the solid state. A brief review of the theory of kinetics for solid state reactions was presented in a paper by Singh.[4] The data were also analyzed with respect to first-order kinetics from the plot of the ln of the molar fractions vs. time. Here, a better linear correlation was observed, thus allowing the determination of well defined, first-order rate constants. Based on these observations, it was decided in all cases to apply first-order kinetics for determination of rate constants for the rearrangements of **3** and **4** in the solid state as well as in the melts.

The experimental results for **3** are compiled in Table 5, while the results for **4** are shown in Table 6. In order to estimate the uncertainties, all experiments were repeated at least three times at each temperature. Quite large deviations were observed. However, these were the best results possible using the described experimental technique. It was difficult to get satisfactory result for each kinetic run. This may be due to shortcomings of the experimental technique. At the same time, for solid state reactions reproducible results are rarely obtained because of the difficulties of obtaining crystals free from imperfections. At high temperatures, e.g., at 253 °C for triazole **4**, reaction times were so short that it was difficult to achieve proper temperature equilibria and obtain well defined reaction times. The uncertainties are reflected by the correlation values (r^2) in the tables.

Table 5. Thermolysis of 4-ethyl-3,5-diphenyl-4*H*-1,2,4-triazole, **3**, (m.p. 160 °C).

	1st order reaction in melt			1st order reaction in crystal		
T/°C	k/s^{-1}	r^2	n^a	k/s^{-1}	r^2	n^a
190	7.44×10^{-5}	0.99	8			
191	8.24×10^{-5}	0.99	9			
189	7.35×10^{-5}	0.99	9			
171	1.86×10^{-5}	0.67	4	7.00×10^{-6}	0.99	4
171	1.45×10^{-5}	0.98	5	5.82×10^{-6}	0.84	4
172	1.83×10^{-5}	0.95	4	4.14×10^{-6}	0.98	4
152	2.47×10^{-6}	0.94	4	6.77×10^{-7}	0.46	2
151	3.11×10^{-6}	0.90	4	5.76×10^{-7}	0.99	3
151	1.66×10^{-6}	0.88	4	4.26×10^{-7}	0.90	3
141	1.36×10^{-6}	0.95	4	1.47×10^{-7}	0.99	4
141	2.65×10^{-6}	0.98	5	2.44×10^{-7}	0.86	3
140	2.38×10^{-6}	0.95	4	2.19×10^{-7}	0.95	4
131				4.19×10^{-8}	0.85	5
130				3.42×10^{-8}	0.86	5
129				4.71×10^{-8}	0.83	5

[a] Number of points used in the linear regression.

Table 6. Thermolysis of 4-methyl-3,5-diphenyl-4*H*-1,2,4-triazole, **4** (m.p. 245 °C).

	1st order reaction in melt			1st order reaction in crystal		
T/°C	k/s^{-1}	r^2	n^a	k/s^{-1}	r^2	n^a
253	1.05×10^{-2}	0.87	9			
255	7.10×10^{-3}	0.49	9			
254	1.10×10^{-2}	0.97	8			
254	2.84×10^{-2}	0.95	7			
253	2.09×10^{-2}	0.91	9			
234	6.94×10^{-3}	0.78	3	5.16×10^{-4}	0.62	4
235	7.06×10^{-3}	0.90	3	7.00×10^{-4}	0.94	4
235	6.75×10^{-3}	0.75	3	4.62×10^{-4}	0.74	4
214	1.78×10^{-3}	0.54	4	2.35×10^{-4}	0.97	5
215	1.73×10^{-3}	0.90	4	2.69×10^{-4}	0.78	5
214	1.65×10^{-3}	0.72	4	2.40×10^{-4}	0.92	5
195	1.13×10^{-3}	0.61	4	7.13×10^{-5}	0.98	4
195	–		2	7.61×10^{-5}	0.95	5
194	1.63×10^{-3}	0.93	3	6.14×10^{-5}	0.98	5

[a] Number of points used in the linear regression.

Despite these limitations the results clearly illustrate the processes taking place. A typical example is illustrated by Fig. 6. This is a plot of ln(molar fraction) vs. time for the thermolysis of crystals of **4** at 214 °C, i.e. below the m.p. of 245–247 °C. This plot clearly illustrates the existence of two rate constants, one for the rearrangement in the crystals, corresponding to the lower part of the curve, and one due to the reaction in the melt corresponding to the steeper, upper part of the curve. After approx. 10–15% conversion, as expected, the crystals started to melt, as also indicated by the intermittent region of the diagram. Visual inspection of each sample showed that for the lower part, samples still consisted of crystals, with no noticeable changes of the appearance of the crystals. The corresponding curve for thermolysis in the melts, as expected, exhibited no break point, but only the part corresponding to the upper, steep part of the curve in Fig. 6. The rate of reaction was in general approx. 10 times slower in the rigid crystalline state than in the melts.

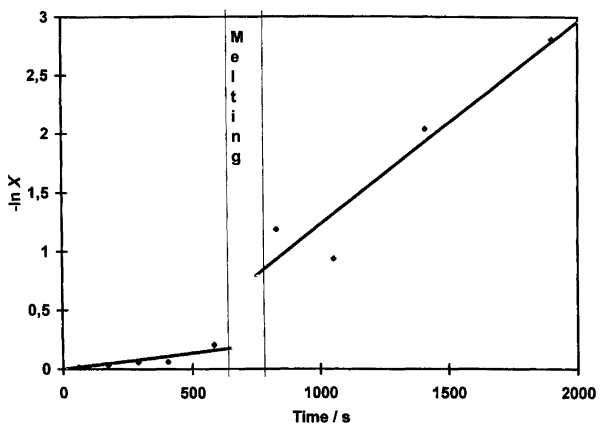

Fig. 6. Thermolysis of **4** at 214 °C, (m.p. 245–247 °C).

Interestingly, when thermolysis of **3** was performed at temperatures slightly higher than the m.p. of the triazoles, the kinetic diagrams exhibited a form similar to that in Fig. 6. This can be rationalized by assuming that even after melting, the samples exist in an ordered structure somewhat resembling the crystal structure.

The rate constants were determined for a number of temperatures. Activation parameters were derived from the variation of ln k_1 vs. $1/T$, where T is the thermodynamic temperature. Thus, for compounds **3** and **4** reasonable Arrhenius fits were obtained as shown in Figs. 7 and 8, respectively. Two lines were obtained, corresponding to reactions in the crystals and the melts, respectively. They were almost parallel for compound **3** while they converged at high temperature for **4**. This reflected differences in activation energies. The activation parameters were calculated using the program LSTSQ (Serena Soft-Ware, Bloomington, Indiana, USA) and are shown in Table 7.

For both compounds activation energies were higher in the crystals than in the melts. The activation energy in the crystals was higher for **3** (173 kJ mol^{-1}) than for **4** (104 kJ mol^{-1}). This difference was in agreement with the experimental crystal structure. The interatomic distances in the crystals between the reacting atoms were larger for **3** (4.6 Å) than for **4** (3.2 Å). Thus, the structure of **4** was closer to the ideal transition state for an S_N2-type group transfer, which was also reflected by the calculated activation entropies which were lower for **4**, ($\Delta S^{\ddagger} = -115$ J mol^{-1} K^{-1}) than for **3**, ($\Delta S^{\ddagger} = -32$ J mol^{-1} K^{-1}.) The transition state was easier to reach in the less regid melts. Therefore, not only were the activation energies lower, but also the $\Delta S^{\ddagger}$-values, e.g., for **4**, -124 J mol^{-1} K^{-1} in the melt vs. -115 J mol^{-1} K^{-1} in the solid strate.

The good agreement with first-order kinetics did not necessarily reflect a unimolecular reaction, but may rather be the result of the rate behavior of a more complex reaction, which cannot be expressed by a single rate expression. The kinetics, however, were in agreement with the Prout–Tompkins equation for solid state reactions using the linear nuclei-growth model.[10] The kinetic, thermodynamic and structural data can be rationalized by a mechanism in which a rate-determining group transfer takes place between neighboring molecules in the crystals. The bulk-rearrangement may now be viewed as a process in which the dialkyltriazolium triazolate initially formed, functions as a catalyst, where the ions react with neighboring, neutral molecules, resulting in formation of the 1-alkyltriazole. This may take place in the same layer occupied by the ions. In the rigid solid state, such a mechanism is, however, less likely, as by this process increased separation of charges will result. An alternative mechanism would be one where the second group transfer (Scheme 1) takes place between the neighboring ions in the salt. This process will, however, require rotation of the triazole rings in the salt, and any larger degree of reorientation, e.g., rotation (here $>120°$) is not likely to take place in the crystal. An alternative rationale would call for the 4-alkyl group transfer to take place from the dialkyltriazolium ion in one layer to the 1-position of a neutral triazole molecule in the next molecular layer, simultaneously with a 4-alkyl group-transfer from a neutral triazole molecule in this layer to the 1-position of the triazolate anion in the first layer. The overall result of such a co-ordinated group-transfer process would be the move of the ion-pair of the salt from one layer to the next, concurrent with formation of the rearranged product.

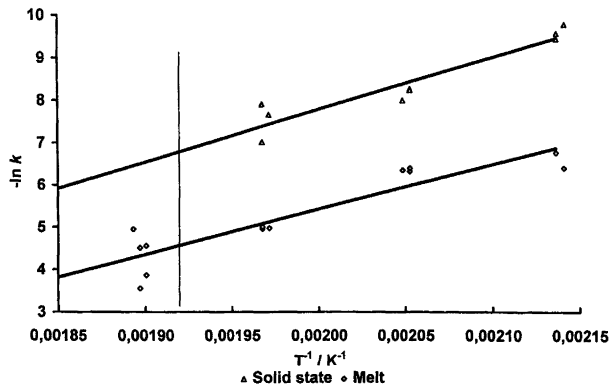

Fig. 7. Thermolysis of **3**.

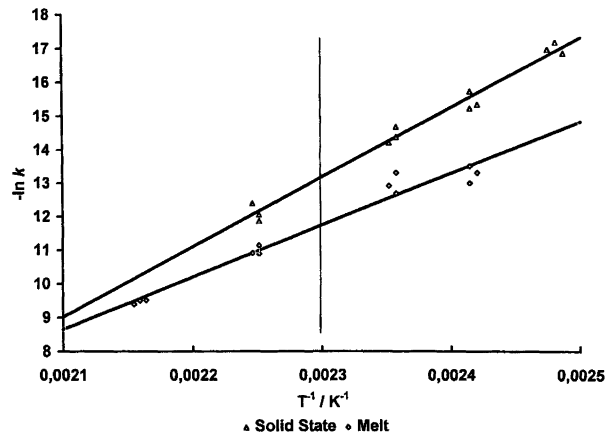

Fig. 8. Thermolysis of **4**.

Table 7. Activation parameters for rearrangement of 4-ethyl- (**3**) and 4-methyl-3,5-diphenyl-4*H*-1,2,4-triazole, **4**.

	Solid state	Melted phase
4-Methyl-3,5-diphenyl-4*H*-1,2,4-triazole **4**		
ln(*A*)	17.2(3.3)	16.1(2.8)
E_a/kJ mol^{-1}	104(13)	89(12)
$\Delta H^{\ddagger}$/kJ mol^{-1}	100(13)	85(12)
$\Delta S^{\ddagger}$/J mol^{-1} K^{-1}	−115(27)	−124(23)
4-Ethyl-3,5-diphenyl-4*H*-1,2,4-triazole **3**		
ln(*A*)	34.7(4.2)	23.8(2.1)
E_a/kJ mol^{-1}	173(14)	128.6(7.7)
$\Delta H^{\ddagger}$/kJ mol^{-1}	170(14)	124.9(7.7)
$\Delta S^{\ddagger}$/J mol^{-1} K^{-1}	−32(35)	−58(18)

In order to find ways to distinguish between these possible mechanistic pathways, we are now searching for 4-alkyl substituted triazoles that do rearrange in the melt but are unreactive in the crystalline state, as the structural characteristics of such compounds may elucidate the critical second steps of the rearranagement mechanism.

References

1. Gautun, O. R. and Carlsen, P. H. J. *Acta Chem. Scand. 46* (1992) 469; Carlsen, P. H. J. and Gautun, O. R. *Acta Chem. Scand. 44* (1990) 485; Bentley, W., Jones, R. V. H. and Wareham, P. J. *Tetrahedron Lett. 30* (1989) 4013; Gautun, O. R. and Carlsen, P. H. J. *Acta Chem. Scand. 48* (1994) 411.
2. Carlsen, P. H. J., Gautun, O. R., Samuelsen, E. J., Mårdalen, J., Helgesson, G. and Jagner, S. *Phys. Scr. 44* (1991) 214.
3. Carlsen, P. H. J., Gautun, O. R., Samuelson, E. J., Helgesson, G. and Jagner, S. *Synth. Met. 38* (1990) 263.
4. Singh, N. B., Singh, R. J. and Singh, N. P. *Tetrahedron 22* (1994) 6441; Kirby, A. J. *Adv. Phys. Org. Chem. 29* (1994) 87.
5. Sukenik, C. N., Bonapace, J. A. P., Mandel, N. S., Lau, P.-Y., Wood, G. and Bergman, R. G. *J. Am. Chem. Soc. 99* (1977) 851; Menger, F. M., Kaiserman, H. B. and Scotchie, L. T. *Tetrahedron Lett. 25* (1984) 2311; Sarma, J. A. R. P. and Dunitz, J. D. *Acta Crystallogr., Sect. B 46* (1990) 780.
6. Gautun, O. R. and Carlsen, P. H. J. *Acta Chem. Scand. 45* (1991) 609.
7. Gilmore, C. J. *J. Appl. Crystallogr. 17* (1984) 42.
8. *International Tables for X-ray Crystallography*, Vol. IV, Kynoch Press, Birmingham 1974.
9. TEXAN *Structure Solution Package*, Molecular Structure Corporation, The Woodlands, Texas 77381, USA 1989.
10. Prout, E. G. and Tompkins, F. C. *Trans. Faraday Soc. 40* (1944) 488.

Received January 24, 1995.